Electrical Engineering (2023) 105:207–219
https://doi.org/10.1007/s00202-022-01660-y

ORIGINAL PAPER

Minimization of torque ripples in PMSM drive using PI- resonant controller-based model predictive control

Suryakant[1,2] · **Mini Sreejeth**[1] · **Madhusudan Singh**[1] · **Aakash Kumar Seth**[1]

Received: 1 October 2021 / Accepted: 26 September 2022 / Published online: 7 October 2022

Abstract
This paper investigates minimization of torque ripples in permanent magnet synchronous motor (PMSM) drive and presents the design and implementation of a proportional-plus-integral resonant (PI-RES) controller-based model predictive control (MPC) of PMSM drive. In MPC, the machine model is used to predict the possible actions of control variables in the time domain and the control operation is then selected based on the optimization of the objective function. In the proposed technique, an objective function is defined by the error between reference current and predicted currents in d–q axis. The objective function is minimized using the MATLAB/Simulink minimum function block for each voltage vector for each sampling interval and provides optimal switching states to control VSI. The PI-RES controller is designed by connecting a variable frequency resonant controller in parallel with a conventional proportional-plus-integral (PI) controller; and is implemented to produce the reference current for MPC of PMSM. The resonant controller generates the compensating torque current, while the PI controller delivers the reference current and establishes the reference torque current. A comparative study of the MPC-based PMSM drive using the classical PI controller and PI-RES controller has been done and the results show the ripples in motor torque are 27.2% and 9.1%, respectively. Simulation analysis shows THD of stator currents are 4.52% & 3.85% at 11 Nm load and 6.53% & 4.4% at load of 5.5 Nm using PI and PI-RES controllers, respectively. Experimental analysis shows that THD of stator currents are 3.10% & 2.29% at 11 Nm load and 8.13% & 5.73% at a load of 5.5 Nm using PI and PI-RES controllers, respectively. The proposed technique shows superior performance over the classical PI controller-based MPC of PMSM drive.

Keywords Permanent magnet synchronous motor · Proportional-plus-integral controller · PI resonant controller · Model predictive control

1 Introduction

PMSMs have been commonly used in variable speed drives for industrial applications, due to their high efficiency, low volume, high torque density and wide range of speed of operation. Of the various methods developed to achieve high performance control of PMSM, vector control (VC) and direct torque control (DTC) are the most significant methods [1]. VC helps to achieve better steady state performance and fast dynamic response in PMSMs over a wide speed range. PMSM has a few inherent limitations, such as machine design imperfections, pulsating torque resulting from effect of dead time, error in current measurement and other uncertainties, especially when motor is used for low-speed operations [2]. The ripples in motor torque can produce speed ripples in the motor, which is not desirable for servo application such as machine tools etc.

Torque dynamics can be improved through use of appropriate control technique. Predictive control technique is one of the widely used techniques, which include deadbeat control (DBC) and MPC techniques [3, 4]. These control techniques can be implemented effectively using digital signal processors (DSP). Dead beat (DB) controller provides good dynamic responses at constant switching frequency as it can force the tracking of a variable to its reference value [5]. Model predictive control (MPC) is a multi-objective control method that is simple to implement and appropriate for nonlinear systems [6]. The use of MPC in the field of power electronics and electrical drives is primarily driven by two

✉ Suryakant
suryakantshukla8@gmail.com

[1] Electrical Engineering Department, Delhi Technological University, Delhi, India

[2] Electrical Engineering Department, National Institute of Technology, Raipur, India

facts: the mathematical models of these systems required by MPC are well understood, and the design of the controller must take into account a number of limitations [7]. The concept of MPC is very intuitive and has the capability to compensate dead time, handle multivariable cases and address nonlinearities [8, 9]. There are two types of MPC: continuous control set MPC (CCS-MPC) and finite control set MPC (FCS-MPC). A modulator is used in CCS-MPC and it runs at constant switching frequency [10]. Model predictive current controller (MPCC) and Model predictive torque controller (MPTC) are the two types of FCS-MPC [11–15]. MPC is adept in predicting the performance parameters like flux, current and torque. In MPTC the control variable are stator flux and motor torque and in MPCC the control variable is defined only in terms of stator current [16, 17]. MPCC is much easier to implement as compared to MPTC as an observer or estimator is required in MPTC to find the value of stator flux and motor torque; while in MPCC current is the control variable that can be measured directly. The tuning of weighting factor is a mandatory requirement for MPTC, which is not the case with MPCC.

PMSM can achieve good control performance when the real-time three-phase current is measured accurately. However, error in measuring the current can produce speed ripples in PMSM drive. Current measurement errors are usually caused by the hall sensor units, the signal processing circuit, analog to digital (A/D) converter and filter circuits [18]. Torque ripples produced due to error in current measurement can be reduced by compensation of the torque generating current. This technique depends on motor variables of machine and is difficult to realize for practical applications.

Speed ripples in motor can be reduced by employing suitable control approach based on principle of internal mode such as repetitive controller [19, 20] and resonant controllers [21, 22]. Repetitive controller has limitation relating to adapting the frequency as it requires variable sampling frequency. Resonant controllers can achieve precise reference tracking and disturbance rejection while producing infinite gain at the unbalanced frequency.

This paper elucidates the design and implementation of a PI-RES speed controller for minimization of torque ripples in MPC-based PMSM drive. The PI-RES controller is designed by connecting a frequency variable resonant controller with PI controller in parallel. The PI-RES controller produces the reference current for MPC of PMSM. The proposed controller produces the reference torque current and is able to reduce ripples by generating compensation torque current from resonant controller along with the main reference current. Simulation studies are carried out to compare the performance of the developed PI-RES controller and the classical PI controller for MPC of PMSM drive. The simulation results are validated on a laboratory prototype using dSPACE ds1104 controller, and it is observed that proposed method improves the overall performance of PMSM drive effectively. The novelty of this paper include:

- An adaptive model predictive controller is developed and implemented as a current controller to find the suitable voltage vectors for the control of the PMSM drive, which provides superior dynamic performance of the drive under various operating conditions.
- A PI-RES controller is designed and implemented in the outer speed loop for MPC of PMSM to ensure reduction in speed ripples.

This paper is structured into six sections including introduction in Sect. 1, Sects. 2, 3, 4, 5, 6, 7, 8 cover Modelling of PMSM, Design of Proposed PI-RES Controller, Principle of proposed MPC of PMSM, Control of PMSM Drive with proposed PI-RES Controller, Simulation Studies and Discussions, Experimental Results followed by Conclusions.

2 Modelling of PMSM

To facilitate simple analysis, the following assumption are made while modelling the PMSM: -

- Magnetic saturation is ignored,
- Back-EMF is assumed to be sinusoidal and
- Cogging torque, hysteresis and eddy current are very small and hence neglected.

The direct and quadrature axes voltages of surface mounted PMSM are [23]:

$$v_d = R_s i_d + L_d \frac{\mathrm{d}i_d}{\mathrm{d}t} - \omega L_q i_q \tag{1}$$

$$v_q = R_s i_q + L_q \frac{\mathrm{d}i_q}{\mathrm{d}t} + \omega L_d i_d + \omega \varphi_m \tag{2}$$

where $v_d, v_q, i_d, i_q, L_d, L_q$ are the d–q axes voltage, current and inductances respectively and $R_s\omega$, φ_m are stator resistance, angular speed, and flux of PMSM, respectively. For a surface mounted PMSM, $L = L_d = L_q$. Hence

$$v_d = R_s i_d + L \frac{\mathrm{d}i_d}{\mathrm{d}t} - \omega L i_q \tag{3}$$

$$v_q = R_s i_q + L \frac{\mathrm{d}i_q}{\mathrm{d}t} + \omega L i_d + \omega \varphi_m \tag{4}$$

The torque dynamics of PMSM is given as:

$$T_e = T_l + J \frac{\mathrm{d}\omega_r}{\mathrm{d}t} + B\omega_r \tag{5}$$

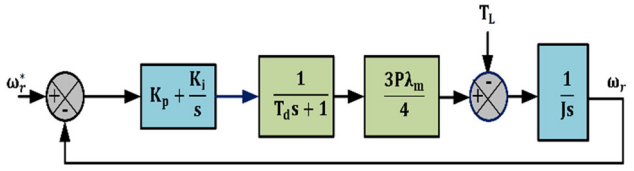

Fig. 1 Outer loop PMSM drive with classical PI speed controller

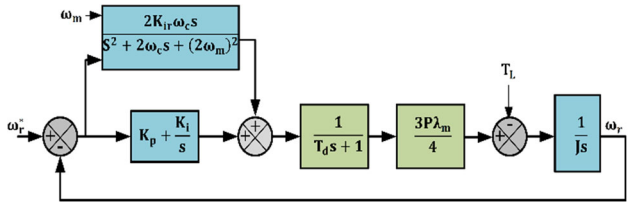

Fig. 2 Outer loop of PMSM drive with PI-RES speed controller

where T_l and T_e are load torque and electromagnetic torque respectively and ω_r, B, J are rotor speed, friction coefficient and moment of inertia, respectively.

T_e can also be represented as

$$T_e = \frac{3}{2} \cdot \frac{P}{2}\left(\varphi_d i_q + \varphi_q i_d\right) \tag{6}$$

where P is number of poles and φ_d, φ_q are $d-q$ axes flux linkages and is defined as

$$\varphi_d = L_d i_d + \varphi_m \tag{7}$$

$$\varphi_q = L_q i_q \tag{8}$$

Using Eq. (5), electromagnetic torque is expressed as

$$T_e = \frac{3}{2}\frac{P}{2}\varphi_m i_q \tag{9}$$

The mechanical speed is expressed as

$$\omega_m = \frac{\mathrm{d}\theta}{\mathrm{d}t} \tag{10}$$

Here ω_m and θ is defined as mechanical speed and rotor position, respectively.

3 Design of proposed PI-RES controller

The outer loop of the PMSM drive with classical PI controller is presented in Fig. 1, where T_d is the inner loop delay, K_p and K_i are the gains of PI controller and ω_r^* is the reference speed.

The expression of proportional resonant (PR) controller to track AC signal in s-domain is [24, 25]

$$G(s)_{\mathrm{PR}} = K_p + \frac{2K_{ir}\omega_{\mathrm{c}} s}{S^2 + 2\omega_{\mathrm{c}} s + \omega^2} \tag{11}$$

where, ω is the regulated signal frequency, ω_{c} is cut off frequency and K_{ir} is the resonance coefficient. The damping coefficient contributes to increasing the bandwidth of centre frequency of ω as well as expand the phase margin of control system. $G(s)_{\mathrm{PR}}$ gives the open loop infinite gain at resonant frequency ω, that promises accurate tracing for oscillating variables at ω when applied in closed loop, similar to the $G(s)_{\mathrm{PI}}$ applied in rotational reference frame of ω. The $G(s)_{\mathrm{PI-res}}$ is designed by connecting $G(s)_{\mathrm{PI}}$ and $G(s)_{\mathrm{PR}}$ in parallel. In this controller only one gain i.e., K_p is required to be tuned [26]

$$G(s)_{\mathrm{PI}} = K_p + \frac{K_i}{s} \tag{12}$$

$$G(s)_{\mathrm{PI-res}} = K_p + \frac{K_i}{s} + \frac{2K_{\mathrm{ir}}\omega_{\mathrm{c}} s}{S^2 + 2\omega_{\mathrm{c}} s + \omega^2} \tag{13}$$

Figure 2 shows the outer loop of PMSM with proposed PI-RES speed controller. Since the controlling perturbation is repeated and with twice the sinusoidal rotor frequency, the proposed PI-RES controller is created by combining a PR controller with a classical PI controller. The proposed controller has good ability to control the harmonics as compared to classical PI controller. Here the resonance word addresses the rotor frequency of second harmonic, that is acquired from position sensors or through sensor-less control techniques. By combining the compensating torque current produced by the resonant controller and reference current generated by the PI controller, the speed ripples are minimized. PI-RES controller generates the reference of pulsating torque current that counter the ripples in load torque.

The motor speed is generally obtained by differentiating the rotor position as shown in (10); however, in this process high frequency noise is produced in discrete systems. A low-pass filter of 500 Hz frequency is employed to reduce this noise in the speed signal.

When the PI-RES controller is employed in the speed loop, the dynamic performance is controlled by K_p,while K_i and K_{ir} remove the error in steady state condition. The phase margin of the speed loop is almost 90° when $K_i = K_{\mathrm{ir}} = 0$ and the system will be stable. The system behaves like a second order system if K_i and K_{ir} are neglected and the speed loop transfer function is expressed as:

$$G_s(s) = K_{\mathrm{ps}} \cdot \frac{1}{\mathrm{Js}} \cdot \frac{1}{T_{\mathrm{d}s} + 1} \cdot \frac{3P\lambda_m}{4} \tag{14}$$

where $T_d = \frac{1}{B_i} + \tau_{\text{LPF}}$. The proportional constant of the speed loop, K_{ps} is:

$$K_{\text{ps}} = \frac{1}{4\delta^2 T_d} \frac{4J}{3P\lambda_m} \tag{15}$$

where δ is the damping coefficient, τ_{LPF} is time constant and B_i is bandwidth of ω.

4 Principle of proposed MPC of PMSM

The basic concept behind the MPC is to use a machine model to predict the possible actions of control variables in the time domain and then select the control operation based on an optimization of objective function. In proposed MPC an objective function is defined as the selection criteria, which selects the optimal switching states fed to the VSI. The estimated values of the variables to be monitored are used to determine the objective function and it is minimized using minimum function block of the MATLAB/Simulink for each voltage vector for each sampling interval. The optimal switching state with the minimum objective function value is chosen and used to control the three-leg VSI. The proposed MPC involves the following three steps: -

(1) Define the objective function.
(2) Build predictive model of inverter and find out its optimal switching states.
(3) Create a prediction model of load.

PMSM being the load on the VSI, a discrete time PMSM model is needed to predict the behavior of variables (such as load current) assessed by the objective functions. The block diagram of MPC algorithm applied in current control method of PMSM drive is presented in Fig. 3.

The stator reference current, i_k^* is obtained from the outer speed loop of PI-RES controller and i_k is measured. For each of the different voltage vectors, the motor's modelling equations are used to predict the value of i_k in the next sampling period (i_{k+1}). The objective function measures the error of predicted and reference currents for the next sampling time. The voltage which produces the minimum value of current error is chosen and applied to the load. The flow chart of the algorithm for implementation of MPC of PMSM is shown as Fig. 4.

The states of the switching are defined as:

$$G = \frac{2}{3}\left(G_a + aG_b + a^2 G_c\right) \tag{16}$$

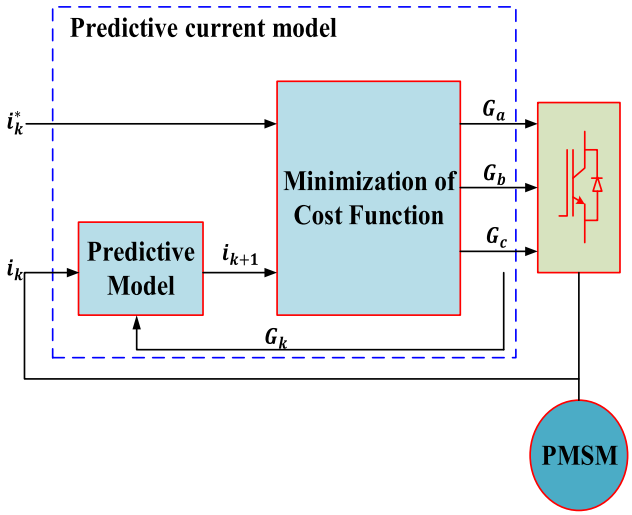

Fig. 3 Scheme for MPC of PMSM

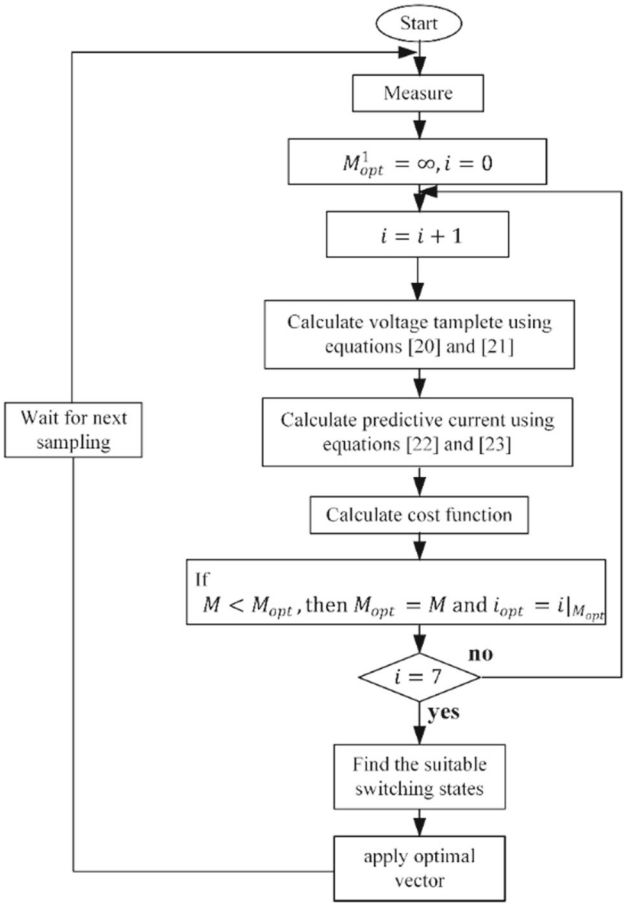

Fig. 4 Flow chart for MPC for PMSM drive

where G_a, G_b and G_c are the pulses given to the inverter and $a = e^{j2\pi/3}$. The output of the inverter is

$$G = \frac{2}{3}\left(v_{an} + a v_{bn} + a^2 v_{cn}\right) \tag{17}$$

Similarly, the current vector, i, and back-EMF, e, of PMSM are expressed as:

$$i = \frac{2}{3}\left(i_a + a i_b + a^2 i_c\right) \tag{18}$$

$$e = \frac{2}{3}\left(e_a + a e_b + a^2 e_c\right) \tag{19}$$

From the modelling equations of PMSM in $d-q$ axes the predictive model is derived as

$$v_q(k) = R_s i_q(k) + \frac{L}{T_s}\left[i_q(k+1) - i_q(k)\right] + L\omega i_d(k) - \varphi_m \omega \tag{20}$$

$$v_d(k) = R_s i_d(k) + \frac{L}{T_s}[i_d(k+1) - i_d(k)] - L\omega i_q(k) \tag{21}$$

$$i_q(k+1) = i_q(k) + \frac{T_s}{L}\left[v_q(k) - R_s i_q(k) - L\omega i_d(k) - \varphi_m \omega\right] \tag{22}$$

$$i_d(k+1) = i_d(k) + \frac{T_s}{L}\left[v_d(k) - R_s i_d(k) + L\omega i_q(k)\right] \tag{23}$$

The objective function, M, for the model predictive control is defined as

$$M = \left|i_{q_{ref}} - i_q(k+1)\right| + \left|i_{d_{ref}} - i_d(k+1)\right| \tag{24}$$

where $i_{q_{\text{ref}}}$ and $i_{d_{\text{ref}}}$ are reference current in d–q axis.

5 Control of PMSM drive with proposed PI-RES controller

Field oriented control (FOC) technique is used to control space vectors of flux, current, and voltage in vector controlled PMSM drive [27, 28]. The block diagram for MPC of a PMSM drive with a PI-RES controller is presented in Fig. 5. The PI-RES controller is used in the outer speed loop to generate reference current depending on the error in reference and motor speeds.

MPC is employed to generate the ideal voltage vector and supplied to inverter. The voltage is chosen and fed to inverter in such a way that the error between reference and predicted current is minimized. Using the observed voltage and current from the inverter, the predicted current for the k^{th} sampling is determined.

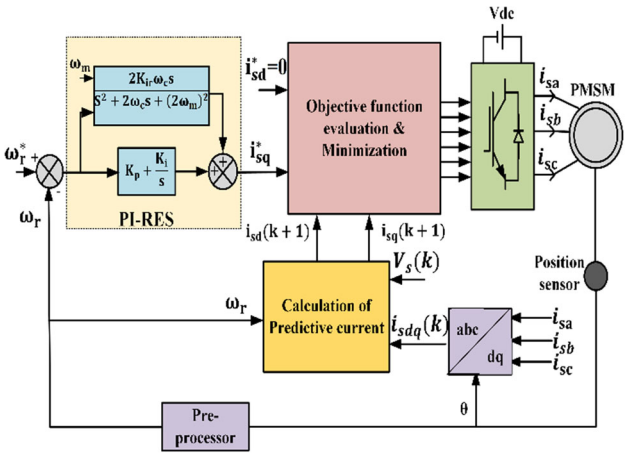

Fig. 5 PMSM drive with PI-RES speed controller

Table 1 Ratings of PMSM

Parameter	Ratings	Parameter	Ratings
Voltage, V	380 V	Rated speed, N	314 rad/s
Current, I	6.9 A	Torque, T	11 Nm
Stator resistance, R_s	1.93 Ω	No. of poles, P	8
L_d&L_q	11.4mH	PM Flux linkage,φ_m	0.265 Wb
Inertia, J	0.11kgm^2		

6 Simulation studies and discussions

The performance of classical PI controller and proposed PI-RES controller for speed control for MPC of PMSM drive are investigated through simulation studies using MATLAB/Simulink, for the motor with specifications as given in Table 1. Load variation, low speed operation, torque ripple analysis and total harmonic distortion (THD) analysis are carried out, with a sampling time of *10* μs for testing of the proposed controller.

A. **Starting characteristics of PMSM drive:**
The starting characteristics of PMSM drive at no-load and rated-speed operation are presented in Fig. 6a, b using PI and proposed PI-RES controller, respectively. Some overshoot and distortion in speed, torque and stator current are observed when PI controller is used as speed controller; while PI-RES controller regulates the speed of the motor without overshoot and gives fast and smooth response.

B. **Dynamic response of PMSM drive during sudden change of load torque:**
Figure 7a, b shows the zoomed dynamic response of the drive during torque transition at rated speed operation

of the motor. The rising time and settling time are also observed to be less with PI-RES controller in comparison with PI controller, which makes the response of the drive faster.

Figure 8 shows the transient characteristics of MPC of PMSM drive at rated speed with PI controller and PI-RES controller, respectively. During starting with no load, some overshoot and undershoot are observed with the PI controller; while PI-RES gives smooth speed characteristics. When the full load is applied at $t = 0.06$ s, speed of the motor settled to the commanded value earlier with PI-RES controller as compared to the PI controller. During the torque transition, the speed perturbation is less in the PI-RES controller.

C. **Dynamic performance of PMSM drive at low-speed operation:**

Figure 9a, b presents the speed, torque and stator current characteristics for MPC of PMSM drive with PI controller and PI-RES controller, respectively, for low-speed (10% of rated-speed) operation. The motor is initially started at a speed of 30 rad/sec under no load condition. The load of rated value i.e., 11 Nm is applied at $t = 0.06$ s to the motor. From Fig. 9a, b it can be seen that when the load is applied to motor an overshoot is observed in torque characteristics of motor. It is also observed that PI-RES controller provide smooth dynamic characteristics of speed, torque and current of MPC of PMSM drive in comparison of PI controller.

Figure 10 presents the zoomed speed characteristics during torque transition for this operating speed. The proposed PI-RES controller reduces the overshoot and undershoot of speed when load torque is applied. In addition, the settling time of motor speed to its reference speed with PI-RES speed controller is less than that of conventional PI speed controller.

D. **Steady state characteristics of PMSM drive:**

The steady state characteristics for MPC of PMSM drive with PI controller and PI–RES controller are shown in Fig. 11a, b, respectively. Some torque ripples are observed in the steady state characteristics. The ripples in motor torque are 27.2% and 9.1% for MPC of PMSM drive with PI controller and proposed PI-RES controller, respectively. Thus, it is evident that the use of PI-RES for MPC of PMSM achieves better torque characteristics, with less ripples during steady state condition, as compared to classical PI controller.

E. **Output response of PI and PI-RES controller**

Figure 12 shows the reference current in q-axis $\left(i_q^*\right)$ for PMSM drive using PI controller and PI-RES controller-based MPC.

It is observed that PI-RES generates reference pulsating torque current that counter the toque ripples in q-axis current of motor and torque of the motor resulting in reduced torque ripples as compared to PI controller.

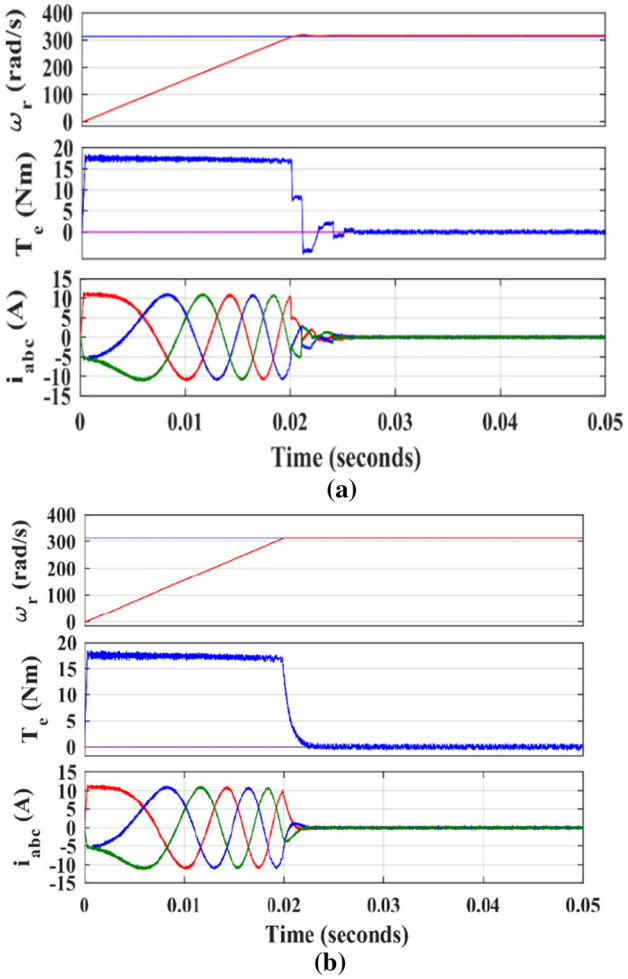

Fig. 6 Starting characteristics for MPC of PMSM drive at rated operation with: **a** PI Controller **b** PI-RES Controller

F. **Stator currents of PMSM drive in d-axis and q-axis**

Figures 13 and 14 show the stator current of PMSM drive using PI controller and PI-RES controller-based model predictive control. At constant torque operation direct axis current is zero and quadrature axis current i_q is proportional to load torque.

It is observed that as the load changes, there is a proportional change in i_q while i_d is maintained at zero for constant torque operation. The ripples in stator current in d–q axis are observed to be less for the PI-RES controller as compared to conventional PI controller, which results in lower torque ripples.

G. **THD in stator current of PMSM:**

Figure 15a, b presents the harmonics spectrum of stator current at full load with PI controller and PI-RES controller, respectively.

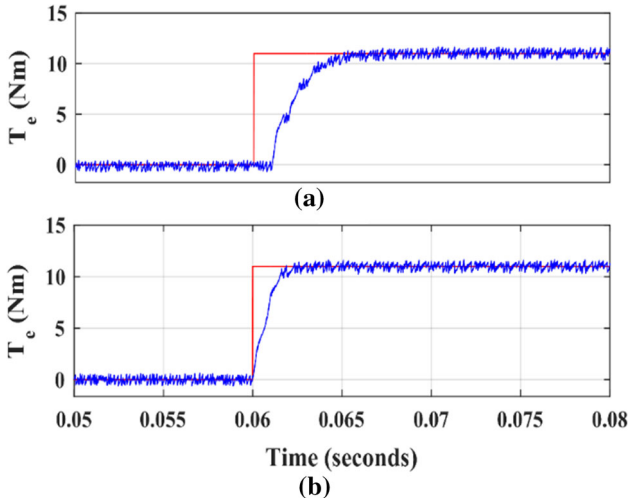

Fig. 7 Torque dynamics for MPC of PMSM during torque transition at rated speed operation: **a** PI Controller **b** PI-RES Controller

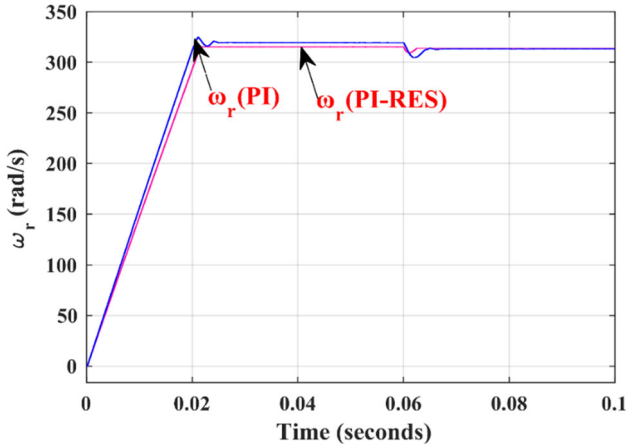

Fig. 8 Transient characteristics for MPC of PMSM Drive at rated speed with: **a** PI Controller **b** PI-RES Controller

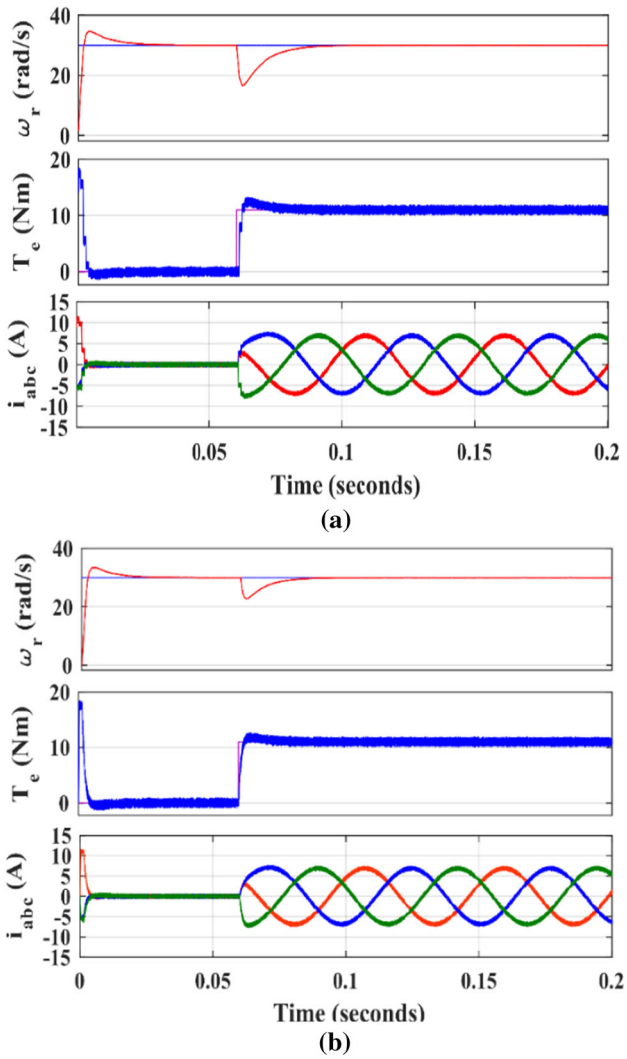

Fig. 9 Dynamic performance for MPC of PMSM at 10% of rated-speed operation with: **a** PI Controller **b** PI-RES Controller

Figure 16a, b presents the harmonics spectrum of stator current at 50% of rated load with PI controller and PI-RES controller, respectively.

The ripples in stator current of the motor are low when the switching frequency is high. The average frequencies of switching in both methods i.e., PI and PI-RES are set similar for the comparative analysis. The THD is analyzed unto 6 kHz for the motor fundamental frequency of 200 Hz. The stator current is selected up to 2 cycles for THD analysis.

Figure 17 shows the comparative results of THD in stator current for load torques of 11 Nm and 5.5 Nm. It is observed that THD in stator current using PI-RES is lower in comparison with that of PI controller.

7 Experimental results

To validate the aforesaid simulation studies, an experimental laboratory prototype for the operation of PMSM drive with different controllers is developed and implemented, which is shown in Fig. 18. The laboratory prototype consists of the dSPACE controller ds1104, VSI, current and voltage sensors, driver circuit and power supplies along with the PMSM. The control method is implemented using a dS1104 TMS320F240 controller board and MATLAB/Simulink. The parameters of PMSM used for the experimental analysis is specified in Table 1. The VSI supplies the stator voltage to the PMSM, which is regulated by gate pulses generated by the dS1104 controller through various control techniques. A DC machine is coupled to PMSM for electrical loading on the PMSM. The two current sensors sense the stator currents

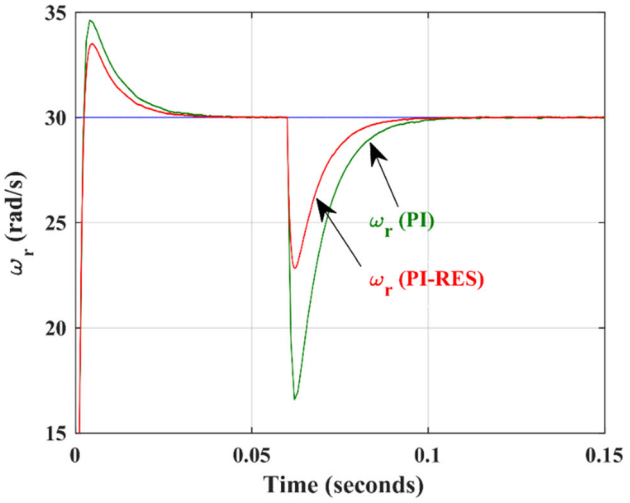

Fig. 10 Zoomed speed-response during torque transition for MPC of PMSM at 10% of rated-speed operation with: **a** PI Controller **b** PI-RES Controller

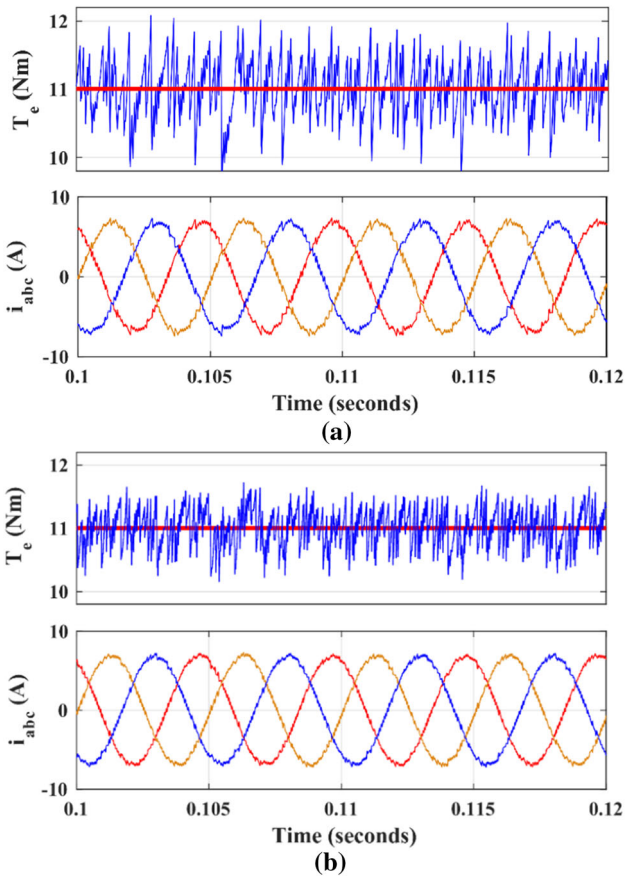

Fig. 11 Steady state characteristics for MPC of PMSM at rated torque operation with: PI **a** Controller **b** PI-RES Controller

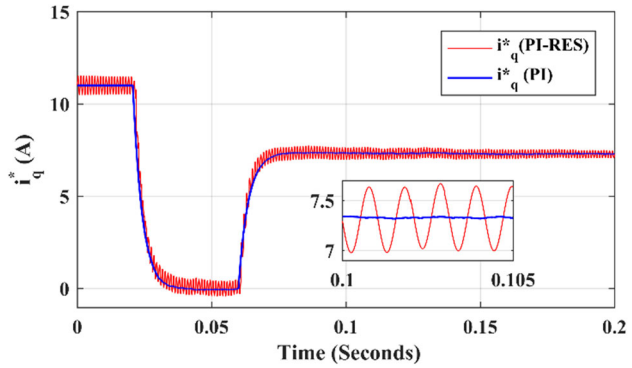

Fig. 12 reference current i_q^* using PI controller and PI-RES controller

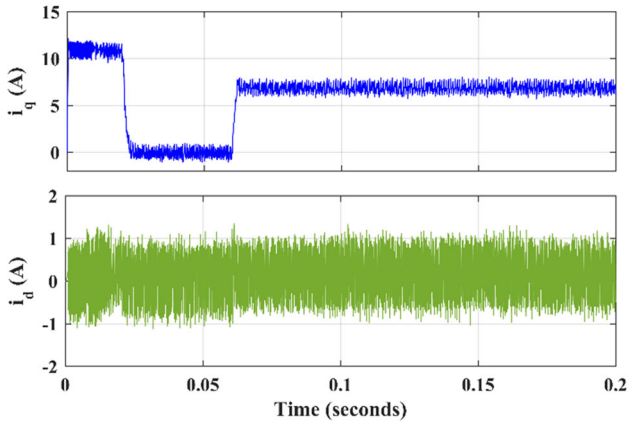

Fig. 13 i_q and i_d of PMSM drive using PI controller-based MPC

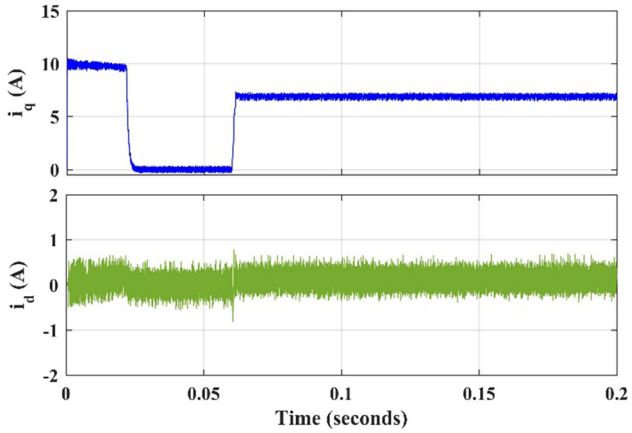

Fig. 14 i_q and i_d of PMSM drive using PI controller-based MPC

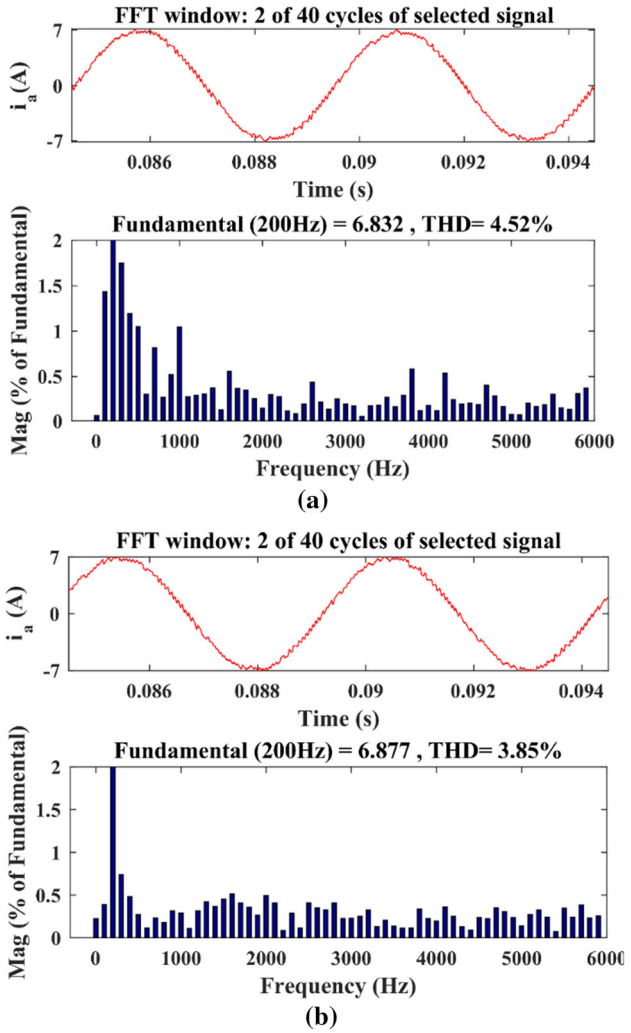

Fig. 15 THD in stator current during rated-load operation with: **a** PI Controller **b** PI-RES controller

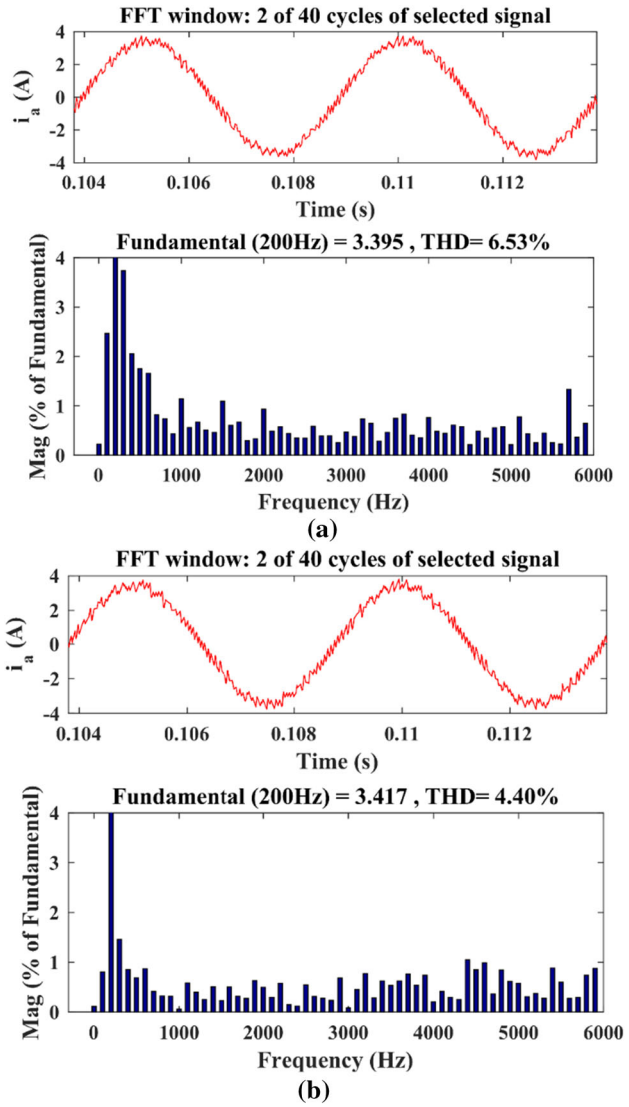

Fig. 16 THD in current during operation at 50% of rated-load with: **a** PI controller **b** PI-RES controller

of PMSM. The sampling time is set to 50 μs for both control techniques.

A. **Performance of PMSM drive during starting under no load condition:**
Figure 19a, b shows the dynamic response for MPC of PMSM drive with conventional PI and PI-RES controllers respectively during starting under no load condition. This includes the motor speed, ω_r, torque, T_e and stator currents, i_{abc}. The PMSM takes a few seconds to reach steady state speed, and the torque generated is sufficient to achieve and maintain the desired rotor speed. The current required by the motor during startup is large to overcome the motor inertia, but gradually decreases to zero load current. The no-load dynamics for the two controllers are similar with the PI-RES controller being slightly faster in achieving steady state condition.

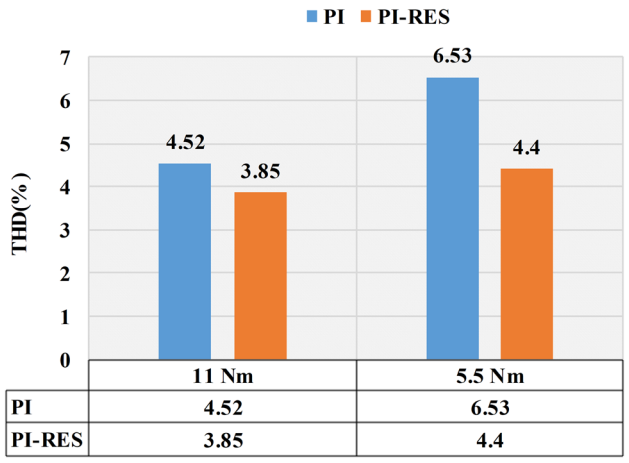

Fig. 17 Comparison of THD in stator current for loads of 11 Nm and 5.5 Nm

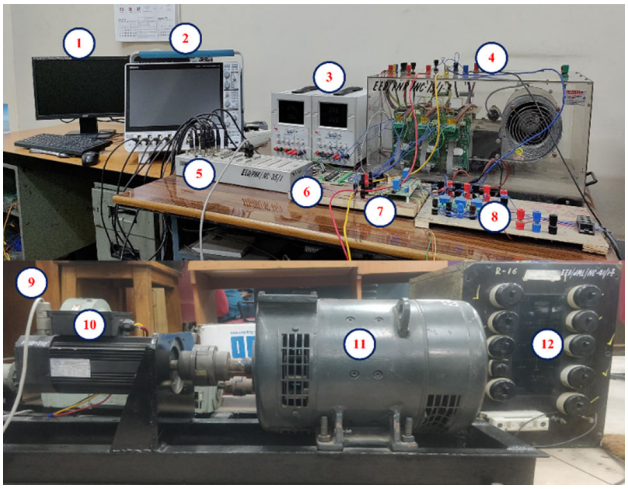

Fig. 18 Developed laboratory prototype of PMSM drive: 1-PC, 2-eight channel MSO, 3- DC power supply, 4- three phase inverter, 5- dSPACE 1104, 6-driver circuit, 7-current sensors, 8-voltage sensors, 9-encoder, 10-PMSM, 11-DC generator, 12-resistive load

B. **Dynamic performance of PMSM drive during low-speed operation:**
Figure 20a, b shows the dynamic performance of the PMSM drive during low-speed operation for MPC of PMSM drive using PI and PI-RES controllers, respectively. The reference speed of the motor is set to 31.4 rad/s. Initially the motor is started at no load and after attaining the steady state condition, a rated load of 11 Nm is applied to the motor. From Fig. 20a, b, it is observed that PI-RES controller has better performance for the MPC of PMSM drive with lesser torque ripples and smooth characteristics as compared to the conventional PI controller.

C. **Performance of PMSM drive during steady state condition**
Figure 21a, b shows the torque, T_e and stator currents, i_{abc} for MPC of PMSM drive during steady-state condition with rated load using PI and PI-RES controllers. The motor is started at no-load and after attaining the desired speed, the rated load of 11 Nm is applied to the PMSM. It is observed that the torque ripples are less in the developed torque for the PI-RES controller as compared to the PI controller.

D. **THD analysis of stator currents of PMSM drive**

Figures 22 and 23 show the harmonic spectrum of stator current i_a for MPC of PMSM drive using PI and PI-RES controllers respectively, under rated load operation and half rated-load operation. The harmonic spectrums are observed up to harmonic order of 40 with a fundamental frequency of 200 Hz. From Fig. 22a, b it is observed that THD in stator current of PMSM at rated load, i.e., 11 Nm, are 3.097%

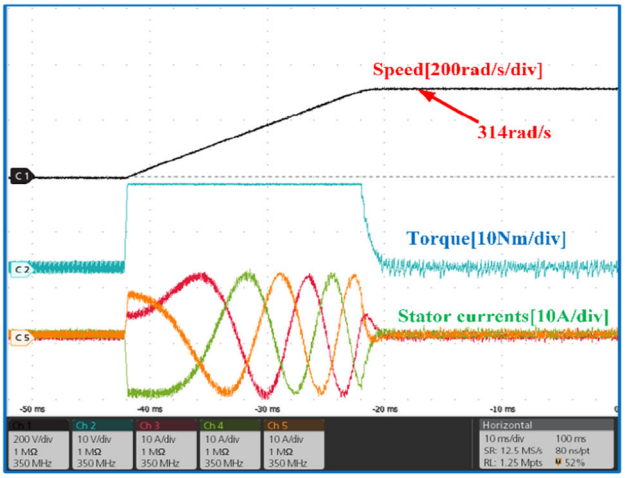

Fig. 19 Dynamic response of PMSM drive during Starting under no load condition using: **a** PI controller **b** PI-RES controller

and 2.286% with PI and PI-RES controllers, respectively. While THD in stator current of PMSM at half rated-load, i.e., 5.5 Nm are 8.125% and 5.717% with PI and PI-RES controllers respectively, which are shown in Fig. 23a, b. It is observed that THD in stator current of PMSM is less with PI-RES controller as compared to the conventional PI controller. The comparative results of THD in stator current of PMSM with PI and PI-RES controller are shown in Fig. 24.

8 Conclusions

A PI-RES controller is designed and implemented for MPC of PMSM drive to regulate the speed and minimize the torque ripples. The performance of the proposed controller is validated by comparing it with the classical PI controller. The

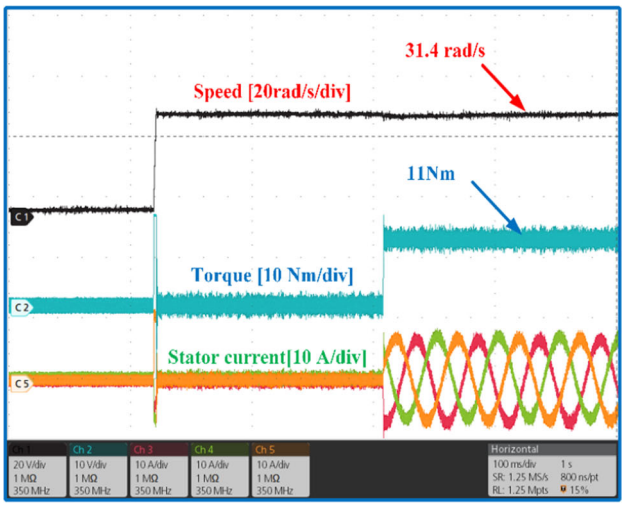

Fig. 20 Dynamic performance of PMSM drive during low-speed operation at rated load condition using: **a** PI controller **b** PI-RES controller

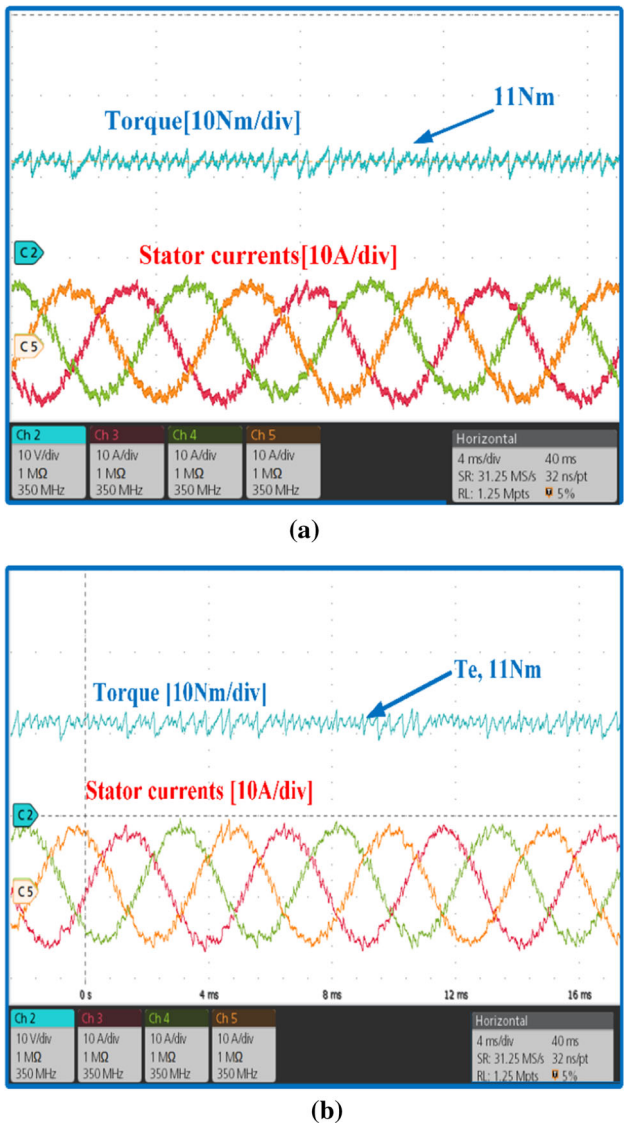

Fig. 21 Performance of PMSM drive during steady state condition using: **a** PI Controller **b** PI-RES Controller

results of simulation studies verified that the proposed controller provides superior dynamic performance compared to the conventional PI controller in terms of starting characteristics, low-speed operation, and transient characteristics. The simulation studies were validated through the developed experimental laboratory prototype based on dSPACE 1104 DSP controller. It is observed that the proposed PI-RES controller-based MPC has several advantages over the PI controller-based MPC of PMSM.

a) The ripples in motor torque with simulation study are observed as 27.2% and 9.1% for MPC of PMSM drive with PI controller and proposed PI-RES controller, respectively, which validates that the proposed method can reduce ripples in the motor torque.

b) THDs are calculated as 4.52% & 3.85% at 11 Nm load and 6.53% & 4.4% at the load of 5.5 Nm using PI and PI-RES controller, respectively, with simulation, while 3.10% & 2.29% at 11 Nm load and 8.13% & 5.73% at the load of 5.5 Nm using PI and PI-RES controller respectively are observed with experimental analysis. Thus proposed method has significantly less THD in stator current at different loads.

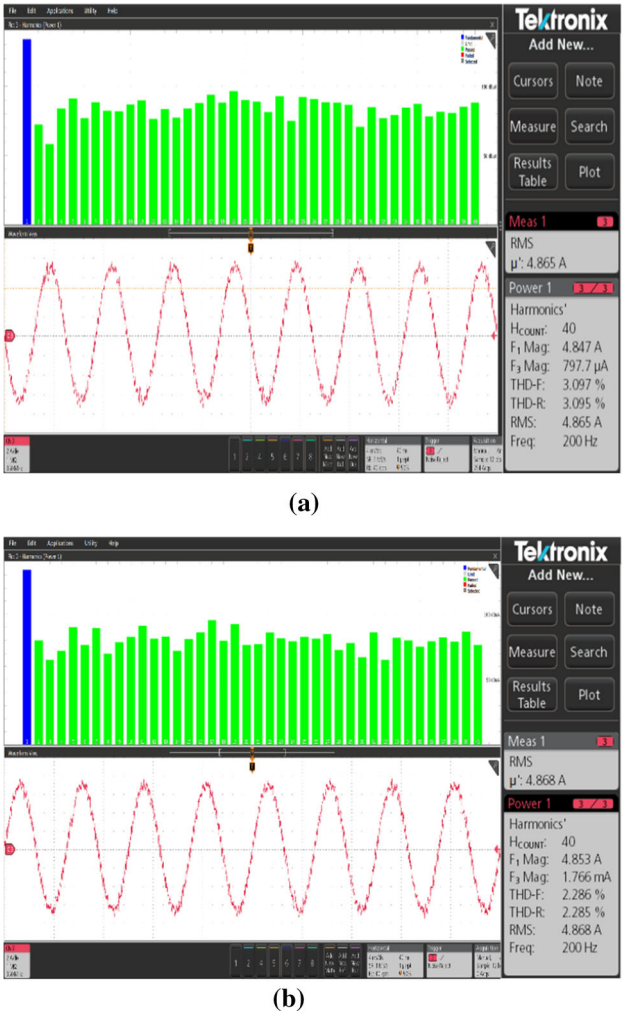

Fig. 22 Harmonic spectrum of stator current of PMSM at rated load using: **a** PI controller **b** PI-RES controller

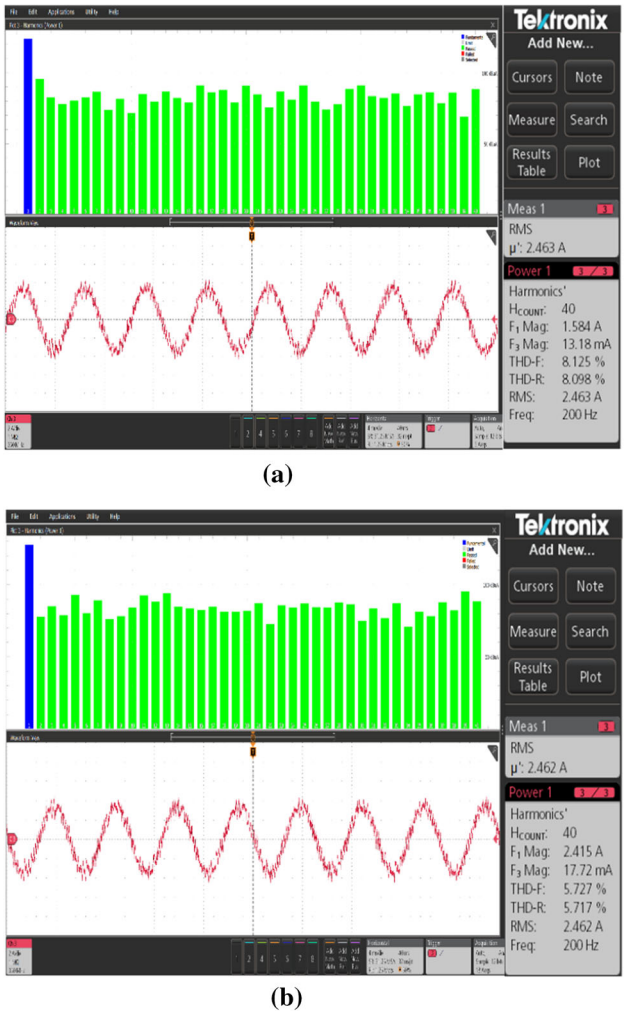

Fig. 23 Harmonic spectrum of stator current of PMSM at half rated-load using: PI **a** controller **b** PI-RES controller

The proposed drive may be useful for industrial applications without torque-ripple, such as spindle drives and accurate positioning systems. In the future proposed technique may also be implemented for electric vehicle applications, which require less ripples in torque by suitably addressing the assumptions related to magnetic saturation, cogging torque etc.

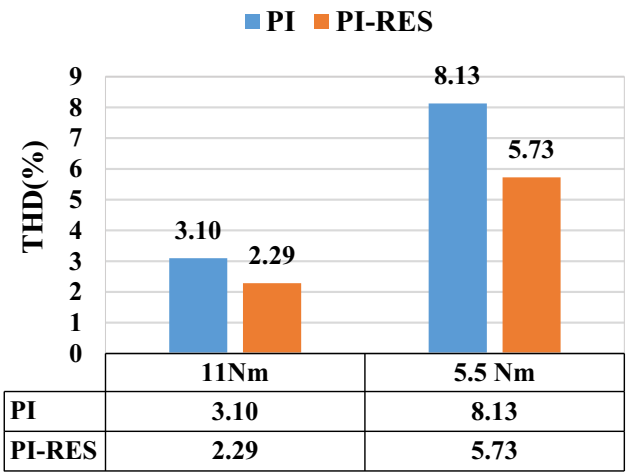

	11Nm	5.5 Nm
PI	3.10	8.13
PI-RES	2.29	5.73

Fig. 24 Experimental results of THD in stator current for loads of 11 Nm and 5.5 Nm

References

1. Casadei D, Profumo F, Serra G, Tani A (2002) FOC and DTC: two viable schemes for induction motors torque control. IEEE Trans Power Electron 17(5):779–787
2. Lee K, Kim S (2019) Dynamic performance improvement of a current offset error compensator in current vector-controlled SPMSM drives. IEEE Trans Ind Electron Sept 66(9):6727–6736
3. Rodrigue JZ, Cortes P (2012) Predictive control of power converters and electrical drives. Wiley, New York
4. Shukla S, Sreejeth M, Singh M (2021) Minimization of ripples in stator current and torque of PMSM drive using advanced predictive current controller based on deadbeat control theory. J Power Electron 21(1):142–152
5. Alexandrou AD, Adamopoulos NK, Kladas AG (2016) Development of a constant switching frequency deadbeat predictive control technique for field-oriented synchronous permanent-magnet motor drive. IEEE Trans Ind Electron 63(8):5167–5175
6. Preindl M, Bolognani S (2013) Model predictive direct torque control with finite control set for PMSM drive systems, part 1: maximum torque per ampere operation. IEEE Trans Ind Inf 9(4):1912–1921
7. Vazquez S, Leon JIL, Franquelo G, Rodriguez J, Young HA, Marquez A, Zanchetta P (2014) Model predictive control: a review of its applications in power electronics. IEEE Ind Electron Mag 8(1):16–31
8. Sandre-Hernandez O, de Jesus R-M, Morales- CR (2019) Modified model predictive torque control for a PMSM-drive with torque ripple minimization. IET Power Electron 12(5):1033–1042
9. Chen J, Qin Y, Bozorgi AM, Farasat M (2020) Low complexity dual-vector model predictive current control for surface-mounted permanent magnet synchronous motor drives. IEEE J Emerg Sel Top Power Electron 8(3):2655–2663
10. Zanelli A, Kullick J, Eldeeb HM, Frison G, Hackl CM, Diehl M (2022) Continuous control set nonlinear model predictive control of reluctance synchronous machines. IEEE Trans Control Syst Technol 30(1):130–141
11. Gong C, Hu Y, Ma M, Yan L, Liu J, Wen H (2020) Accurate FCS model predictive current control technique for surface-mounted PMSMs at low control frequency. IEEE Trans Power Electron 35(6):5567–5572
12. Karamanakos P, Geyer T (2020) Guidelines for the design of finite control set model predictive controllers. IEEE Trans Power Electron 35(7):7434–7450
13. Zhang Y, Xu D, Liu J, Gao S, Xu W (2017) Performance improvement of model-predictive current control of permanent magnet synchronous motor drives. IEEE Trans Ind Appl 53(4):3683–3695
14. Han Y, Gong C, Yan L, Wen H, Wang Y, Shen K (2020) Multi objective finite control set model predictive control using novel delay compensation technique for PMSM. IEEE Trans Power Electron 35(10):11193–11204
15. Niu S, Luo Y, Fu W, Zhang X (2020) An indirect reference vector-based model predictive control for a three-phase PMSM motor. IEEE Access 8:29435–29445
16. Englert T, Graichen K (2018) Nonlinear model predictive torque control of PMSMs for high performance applications. Control Eng Pract 81:43–54
17. Lalezar G, Nejad SMS, Mojiri M (2020) Applying a modified model predictive current control method to improve surface-mounted permanent magnet synchronous motor drives performance in transient and steady-state operations. IET Electr Power Appl 14(10):1886–1897
18. Myers GP, Degner MW (2006) Compensation method for current-sensor gain errors: US, US6998811[P]
19. Zhou K, Yang Y, Blaabjerg F, Wang D (2015) Optimal selective harmonic control for power harmonics mitigation. IEEE Trans Ind Electron Feb 62(2):1220–1230
20. Cui P, Wang Q, Zhang G, Gao Q (2018) Hybrid fractional repetitive control for magnetically suspended rotor systems. IEEE Trans Ind Electron 65(4):3491–3498
21. Gao J, Wu X, Huang S, Zhang W, Xiao L (2017) Torque ripple minimization of permanent magnet synchronous motor using a new proportional resonant controller. IET Power Electron 10(2):208–214
22. Zhou Z, Xia C, Yan Y, Wang Z, Shi T (2018) Disturbances attenuation of permanent magnet synchronous motor drives using cascaded predictive-integral-resonant controllers. IEEE Trans Power Electron 33(2):1514–1527
23. Mohamed YA-RI (2007) Design and implementation of a robust current-control scheme for a PMSM vector drive with a simple adaptive disturbance observer. IEEE Trans Industr Electron 54(4):1981–1988
24. Qiaofen Z, Haohao G, Chen G, Yancheng L, Wang Dong Lu, Kaiyuan ZZ, Xuzhou Z, Dunzhi C (2021) An adaptive proportional-integral-resonant controller for speed ripple suppression of PMSM drive due to current measurement error. Int J Electr Power Energy Syst 129:106866
25. Xia C, Ji B, Yan Y (2015) Smooth speed control for low-speed high-torque permanent-magnet synchronous motor using proportional–integral–resonant controller. IEEE Trans Ind Electron 62(4):2123–2134
26. Yepes AG, Freijedo FD, Lopez O et al (2011) High-performance digital resonant controllers implemented with two integrators. IEEE Trans Power Electron 26(2):563–576
27. Krishnan R, Beutler AJ (1985) Performance and design of an axial field permanent magnet synchronous motor servo drive. In: Proc. IEEE IAS Annu Meeting pp 634–640
28. Lajoie-Mazenc M, Villanueva C, Hector J (1985) Study and implementation of hysteresis controlled inverter on a permanent magnet synchronous machine. IEEE Trans Ind Appl 21(2):408–413